

Histological study on the possible therapeutic role of bone marrow derived mesenchymal stem cells in a model of *Schistosoma mansoni* infestation of spleen of mice

Original
Article

Mona H. Raafat, Sara Abdel Gawad, and Heba Fikry

Department of Histology & Cell Biology, Faculty of Medicine, Ain Shams University, Cairo, Egypt.

ABSTRACT

Background: Hepatosplenomegaly is a characteristic feature of *Schistosoma* infestation. However, splenic injury had received little scientific researches than the well-known liver injury. Moreover, the role of bone marrow derived mesenchymal stem cells (BMMSCs) in treatment of splenic injury due to schistosomiasis has not yet been investigated.

Aim of the work: To explore the structural changes which might occur to spleen during chronic infestation with schistosomiasis and the possible therapeutic role of (BMMSCs) in ameliorating these changes.

Materials & Methods: Fifty female Swiss Albino mice, weighing about 25 gm were classified into group A (control group) and group B (experimental group). Animals in group A were equally subdivided into subgroup AI which served as donors for stem cells obtained from their bone marrow, and subgroup AII which were injected with phosphate buffer saline (PBS) and used to collect control spleen samples. Whereas, animals in group B, were all infected with *S. mansoni* cercariae (60/mouse) by subcutaneous injection, then subdivided into three subgroups; subgroup BI sacrificed after eight weeks, subgroup BII treated intraperitoneally with 2×10^6 MSCs suspended in PBS per mouse at eighth week after infestation then sacrificed four weeks later, and subgroup BIII allowed to survive for twelve weeks without treatment then sacrificed.

Results: Histological examination of spleen sections of subgroup BI showed structural changes including deposition of eggs which were surrounded by inflammatory cells and collagen fibers. Subgroup BIII showed more extensive structural changes. This was associated with significant increase in collagen fibers and TNF- α immunological reaction compared to control. However, (BMMSCs) treated subgroup BII illustrated improvement of splenic structure.

Conclusions: Chronic *Schistosoma mansoni* infestation has a deleterious effect on the structure of the spleen. Bone marrow derived mesenchymal stem cells have a relevant therapeutic potential on the spleen of an animal model of *Schistosoma mansoni*.

Key Words: Bone marrow mesenchymal stem cells, Histology, Mice, *Schistosoma mansoni*, Spleen

Revised: 5 June 2017, **Accepted:** 17 August 2017

Corresponding Author: Mona H. Raafat, **Tel.:** 0201005223587, **E-mail:** raafat.mona@yahoo.com, Department of Histology, Faculty of Medicine, Ain Shams University, Cairo, Egypt

ISSN: 1110-0559, September Vol. 40, No. 3

INTRODUCTION

Schistosomiasis is a complex of acute and chronic infestations caused by a flatworm of the genus *Schistosoma* that is widespread in tropical and sub-tropical environments^[1]. According to WHO, schistosomiasis is the second most socioeconomically devastating parasitic disease (malaria as the first), and schistosome is among the top ten most important agents causing more deaths^[2]. An estimated 779 million individuals are at risk of schistosomiasis and more than 200 million are infected, yet schistosomiasis is often neglected^[3]. In Egypt, the disease is well established and it is estimated that up to 70% of the rural population in endemic areas is affected by *Schistosoma mansoni*^[4]. Considering the spleen as one of the major organs affected during the chronic severe form of schistosomiasis, significant alterations in its morphology become a relevant investigation.

The most commonly used therapeutic drug used in schistosomiasis is praziquantel (PZQ)^[5]. Although, some studies documented that there were (PZQ)-resistant *Schistosoma* strains^[6]. Moreover, it was reported that PZQ induced hemorrhage in the lung tissue of the host^[7]. Therefore, there is a vital need to develop alternative effective drugs to control schistosomiasis without side effects^[8]. Mesenchymal stem cells (MSCs)-based cell therapy has generated a huge amount of attention during the last few years. Stem cell therapy is a kind of intervention strategy that introduces new cells into damaged tissues, which help in treating many diseases and injuries^[9]. It has been proved that stem cell therapy is effective for the treatment of cancers^[10], diabetes mellitus^[11], Parkinson's disease^[12], cardiovascular diseases^[13], and neurological disorders^[14]. Recently, stem cell therapy has been introduced to treat parasitic infestation in animal models, and satisfactory outcomes are achieved^[15]. Although,

probably no studies were performed up to the time of this work on the effect of (MSCs) on the treatment of splenic injury induced by *Schistosoma mansoni*.

Thus, the aim of this study was to explore the morphological changes which might occur to spleen during chronic infestation with schistosomiasis and the possible therapeutic role of (MSCs) in ameliorating these changes.

MATERIALS AND METHODS

The experiment was performed in the Schistosome Biological Material Supply Center of Theodor Bilharz Research Institute (TBRI), Giza, Egypt. The laboratory animals were treated in accordance with the valid International Guidelines for animal experimentation. Fifty female Swiss Albino mice, 7 weeks old, weighing about 25 gm were kept in standard housing conditions and were given food and tap water ad libitum. Animals were classified into group A (control group, n=20) and group B (experimental group, n=30). Animals in group A were equally subdivided into subgroup AI (n=10) which served as donors for stem cells obtained from their bone marrow, and subgroup AII (n=10) which were injected with phosphate buffer saline (PBS) and used to collect control spleen samples. Whereas, animals in group B, were all infested with *S. mansoni* cercariae (60/mouse)^[16] (obtained from infested *Biomphalaria alexandrina* snails which were bred and maintained at the TBRI), injected subcutaneously then subdivided into three subgroups; subgroup BI (n=10) sacrificed after eight weeks, subgroup BII (n=10) treated intraperitoneally with 2×10^6 MSCs suspended in PBS per mouse at eighth week after infection then sacrificed four weeks later, and subgroup BIII (n=10) allowed to survive for twelve weeks without treatment then sacrificed.

Infestation was certain by finding *S. mansoni* eggs in stool 42 days post infestation.

Preparation and isolation of BM-MSCs:

Bone marrow (BM) cells were collected from mice in subgroup AI by flushing the femurs and tibiae. The isolation process was carried out in a laminar flow cabinet under strict sterile conditions. Extracted BM was suspended in complete medium. A total volume of 100 ml of the medium constituted the following: 80 ml of Dulbecco's modified Eagles medium, 15 ml of fetal bovine serum, and 5 ml of penicillin-streptomycin mixture. The solutions were purchased from Lonza Company (Basel, Switzerland). Bone marrow suspended in the media was then placed in sterile Easy flasks and Petri dishes. The cultured BM cells were incubated in a humidified incubator at 37°C in 5% CO₂ and 95% air. The cultured cells were examined daily with an inverted microscope (Axiovert 100; Carl-Zeiss, Jena, Germany) to follow-up the growth of the cells and to detect any infection. Every third day the supernatant was removed by aspiration using a sterile pipette. The adherent cells in flasks and dishes were then washed

twice with sterile PBS and fresh complete media were added. The MSCs were distinguished by their tendency to adhere to tissue culture plastic. On day 9, the cultured cells showed confluent appearance. The MSCs in flasks were separated using 0.25% trypsin in 1mM EDTA for 5 min at 37 °C. The suspension then was centrifuged, viable and non-viable cells were counted using hemocytometer, followed by subculturing viable cells at 4×10^3 cells/cm², and used for experiments after the third passage. Some dishes with adherent MSCs were fixed using freshly prepared precooled (-20°C) mixture of acetone/methanol at 1: 1, for 10 min at room temperature. The fixed adherent MSCs were stained with Giemsa stain and examined using an inverted microscope. Other dishes with adherent MSCs were characterized using the streptavidin-biotin immunoperoxidase technique for CD44 (positive for MSCs and negative for hematopoietic cells) (dilution 1: 100, purchased from Labvision, New York, New York, USA)^[17].

Histological and immune-histochemical studies:

For light microscopic examination; half of the spleen specimens were fixed in 10% buffered formalin, dehydrated, cleared and embedded in paraffin. Serial 5 µm sections of the spleen were stained with hematoxylin and eosin (H&E), Mallory trichrome stain, immunohistochemical staining for tumor necrosis factor-alpha (TNF-α) polyclonal antibody (dilution 1:200, purchased from Labvision), positive controls using thymus tissue were processed according to the same protocol. CD44 monoclonal antibody (dilution 1:100, purchased from Labvision) as marker for BMMSCs and bone marrow tissue was used as positive control^[18].

For transmission electron microscope (TEM) examination; other half of the spleen specimens were cut (1mm³) and fixed in 2.5% glutaraldehyde solution, followed by 1% osmium tetroxide, dehydrated, and embedded in epoxy resin. Ultrathin sections were collected on copper grids and stained with uranyl acetate and lead citrate^[18]. The ultrastructural examination was carried out with a transmission electron microscope (JEM-1200; Jeol, Akishima-Shi, Tokyo, Japan) at the Faculty of Medicine, El Azhar University.

Morphometric measurements:

Samples were analyzed using an image Leica Q win V.3 program installed on a computer in the Histology and cell biology Department, Faculty of Medicine, Ain Shams University. The computer was connected to a Leica DM2500 microscope with built-in camera (Leica Microsystems GmbH, Ernst-Leitz-Strasse, Wetzlar, Germany). Ten specimens from ten different mice of each subgroup were examined (n=10). From each specimen, five different captured non-overlapping fields were taken. Five different readings from every captured photo were counted and the mean was calculated for each specimen. Measurements were taken by an independent observer

blinded to the specimens' details so as to perform an unbiased assessment.

The following parameters were measured:

(1) The mean of area percentage of collagen fibers using Mallory trichrome stain.

(2) The mean count of (TNF- α) positive brownish cells.

All the measurements were taken at high-power fields of magnification ($\times 400$).

Statistical analysis:

All data were collected, revised, and subjected to statistical analysis using one-way analysis of variance performed with SPSS.21 program (IBM Inc., Chicago, Illinois, USA) analysis for variance (ANOVA)-one way analysis and post-Hoc least significant difference (LSD). The significance of the data was determined by the P value. P values greater than 0.05 were considered non-significant, and P values less than 0.05 were considered significant. Summary of the data was expressed as mean \pm standard deviation (SD).

RESULTS

Primary culture of bone marrow-derived mesenchymal stem cells results:

Examination of primary culture of BMMSCs using an inverted light microscope showed on day 5, most of attached cells had cytoplasmic processes and with vesicular nuclei (Fig. 1). On day 9, the attached cells appeared forming colonies with granular cytoplasm and interdigitating processes (Fig. 2). On using Giemsa stain, the colonies of attached cells on day 9 of tertiary culture appeared with purple cytoplasmic reaction of tertiary culture (Fig. 3). Characterization of cultured cells on day 9 of tertiary culture using CD44 revealed that some of the attached cells of tertiary culture showed positive brownish immune-reaction (Fig. 4).

Histological and morphometric results of the spleen:

Histological examination of H&E stained sections of control spleen of (subgroup AII) showed that the splenic stroma was formed of a capsule and septa while the parenchyma was formed of white pulp scattered irregularly in a background of red pulp (Fig. 5). The white pulp consisted of central arteriole surrounded by many lymphocytes with darkly stained nuclei. The red pulp appeared consisted of splenic cords and blood sinusoids (Fig. 6). Sections of subgroup BI revealed disrupted parenchymal architecture with loss white pulp in some areas while others appeared with irregular arrangement of white pulp. Aggregation of inflammatory cells were seen surrounding *Schistosoma mansoni* degenerated egg (Fig. 7). In addition, there were megakaryocytes and giant

cells in the parenchyma (Fig. 8). Sections of subgroup BII showed irregular capsule and the parenchyma was formed mainly of red pulp with reappearance of few white pulps (Fig. 9). Part of white pulp containing central arteriole and red pulp with splenic sinusoids were apparently similar to the control. (Fig. 10). Meanwhile, sections of subgroup BIII showing *Schistosoma mansoni* worm in a blood vessel in the stroma of the spleen and it was surrounded by numerous inflammatory cells. Thick connective tissue septa are also noticed. (Fig. 11). Moreover, there was dilatation and disruption of the wall of some of the splenic vessels containing eosinophilic material and numerous inflammatory cells (Fig. 12). Many deeply basophilic calcified *Schistosoma mansoni* eggs with noticeable egg shells were present in the splenic parenchyma. Thick connective tissue septa and dilated splenic sinusoids were also detected in some specimens (Fig. 13). Meanwhile, the splenic parenchyma in other specimens was infiltrated with numerous cells with faintly stained nuclei and margination of the chromatin at the nuclear membrane (Fig. 14).

In Mallory trichrome stained sections of control spleen of subgroup AII few collagen fibers were noticed in the capsule and septa (Fig. 15). However, in subgroup BI there was significant increase ($P < 0.05$) in the area percentage of collagen fibers compared to control subgroup AII (Fig. 16) (Table1, Histogram 1). The sections of subgroup BII showed significant decrease ($P < 0.05$) in the area percentage of collagen fibers compared to subgroup BI and BIII (Fig. 17) (Table1, Histogram 1). Meanwhile, sections of subgroup BIII showed significant increase ($P < 0.05$) in the area percentage of collagen fibers compared to all other groups. Moreover, there were subcapsular collagen fibers surrounding many blood sinusoids (Fig. 18) (Table1, Histogram 1).

In immunohistochemical analysis for (TNF- α), sections from the control subgroup AII revealed few scattered cells with positive immune-histochemical reaction (Fig. 19). However, in subgroup BI there was significant increase ($P < 0.05$) in number of cells with positive immune-histochemical reaction compared to control subgroup AII (Fig. 20) (Table1, Histogram 2). The sections of subgroup BII showed significant decrease ($P < 0.05$) in the number of cells with positive immune-histochemical reaction compared to subgroup BI and BIII (Fig. 21) (Table1, Histogram 2). Whereas, sections of subgroup BIII showed significant increase ($P < 0.05$) in the number of cells with positive immune-histochemical reaction compared to all other groups. (Fig. 22) (Table1, Histogram 2).

In immunohistochemical analysis for (CD44), sections of spleen of subgroups AII, BI and BIII showed negative immune reaction (Figs. 23 and 25). However, a positive immune reaction was detected in sections of subgroup BII localized in the red pulp (Fig. 24). Figure of subgroup BI was not presented.

Ultrastructural examination of the spleen of the control subgroup AII showed that the white pulp was formed of many lymphocytes and dendritic cells (Fig. 26). The dendritic cells appeared with eccentric euchromatic nuclei and many cytoplasmic processes containing many granules with heterogenous appearances between the surrounding lymphocytes (Fig. 27). The reticular cells appeared with euchromatic nuclei with their processes surrounding electro-lucent areas (Fig. 28). However, the plasma cells seemed to have euchromatic eccentric nuclei while the cytoplasm illustrated well developed cisternae of rough endoplasmic reticulum (rER) and mitochondria. The cytoplasmic processes of dendritic cells were closely related to plasma cells (Fig. 29). Meanwhile, the spleen in subgroup BI showed active lymphocytes with euchromatic nuclei (Fig. 30). Megakaryocytes exhibited characteristic demarcation zones containing electron dense granules while, eosinophils with their

characteristic oval shaped granules were also perceived (Fig. 31). Cells with euchromatic nuclei and many dilated cisternae of rER were distinguished (Fig. 32). In addition, cells with fragmented nuclei with loss of their nuclear envelope and multiple electron dense granules in their cytoplasm were detected together with cells with small hyperchromatic nuclei (Fig. 33). However, examination of subgroup BII revealed cells with euchromatic nuclei and irregular nuclear membrane and few eosinophils with their characteristic granules. (Fig. 34). Whereas, many secretory cells appeared with euchromatic nuclei and prominent rER. (Fig. 35). Meanwhile, subgroup BIII showed many proliferating lymphocytes and numerous eosinophils (Fig. 36). Myofibroblasts were detected in the capsule and they were lying on a basal lamina. Collagen fibrils and part of eosinophil with its characteristic granules were also noticed (Fig. 37).

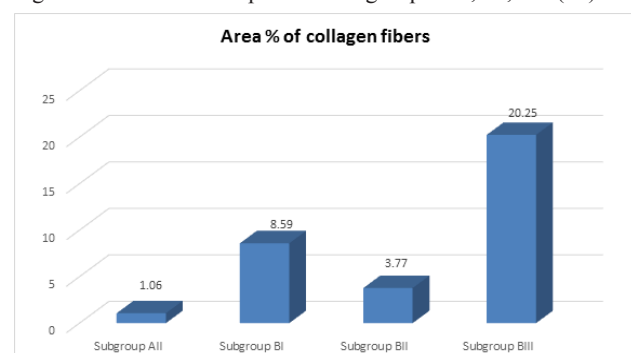
Table 1: Mean \pm SD of area percentage of collagen fibers and mean \pm SD of number of TNF- α positive cells / HPF in different subgroups.

Subgroups	Mean \pm SD of area % of collagen fibers	Mean \pm SD of number of α -TNF positive cells
Subgroup AII	1.06 \pm 0.26	1.8 \pm 0.8
Subgroup BI	8.59 \pm 0.81*	84.6 \pm 7.9*
Subgroup BII	3.77 \pm 0.86* \diamond	20 \pm 3.8* \diamond
Subgroup BIII	20.25 \pm 1.53* \blacktriangle	144 \pm 3.39* \blacktriangle

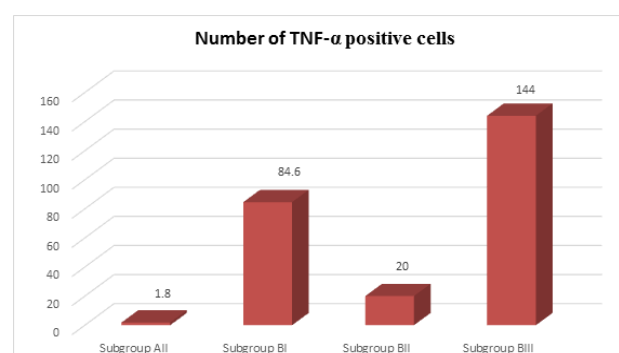
Significant increase compared to subgroup AII (*)

Significant decrease compared to subgroups BI and BIII (\diamond)

Significant increase compared to subgroups AII, BI, BII (\blacktriangle)



Histogram 1. Mean of area percentage of collagen fibers in different subgroups.



Histogram 2. Mean of number of TNF- α positive cells /HPF in different subgroups.

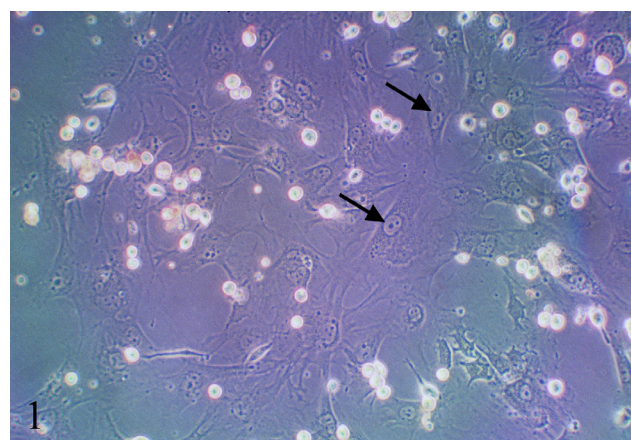


Fig. 1: Primary culture of BMMSCs on day five showing most of the attached cells have cytoplasmic processes and with vesicular nuclei (\uparrow). Inverted microscope X 200.

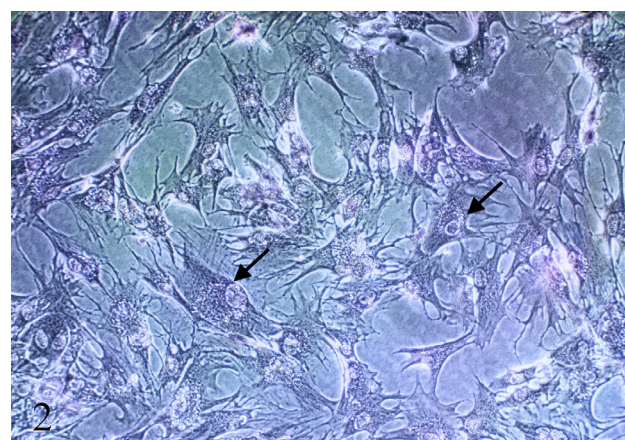


Fig. 2: Primary culture of BMMSCs on day nine showing attached cells forming colonies with granular cytoplasm and interdigitating processes (\uparrow). Inverted microscope X 200.

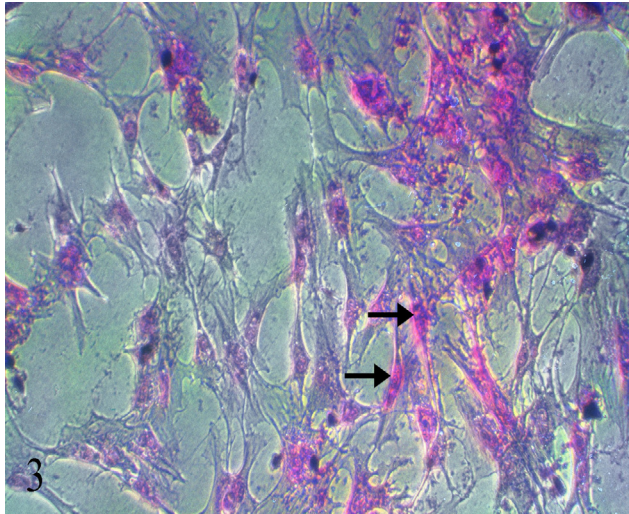


Fig. 3: Tertiary culture of BMMSCs on day nine showing colonies of attached cells. They have purple cytoplasmic reaction (↑). Inverted microscope, Geimsa X 200.

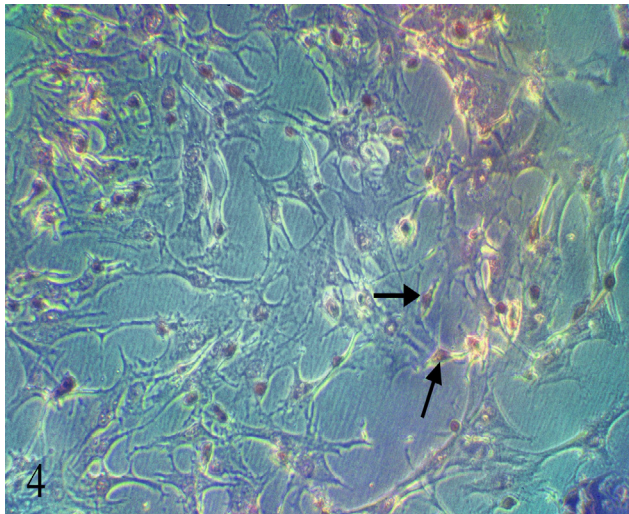


Fig. 4: Tertiary culture of BMMSCs on day nine showing some of the attached cells exhibit positive brownish immune-reaction for CD-44 (↑). Inverted microscope, Streptavidin-biotin peroxidase X 200.

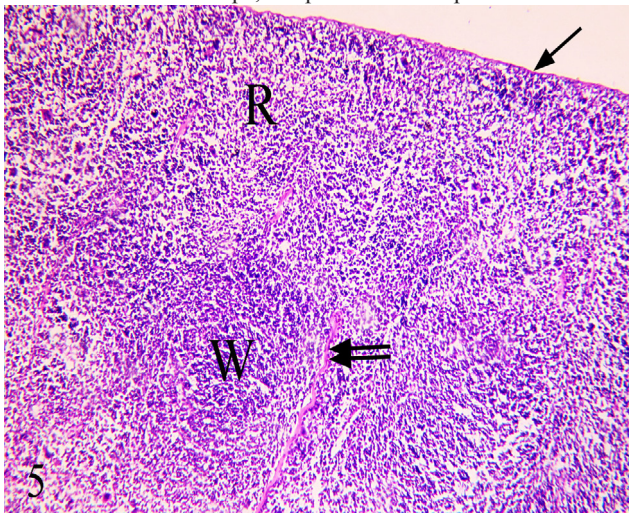


Fig. 5: A photomicrograph of a section of spleen of subgroup All showing capsule (↑) and septa (↑↑). The parenchyma consists of white pulp (W) scattered irregularly in a background of red pulp (R). H&E. X 100.

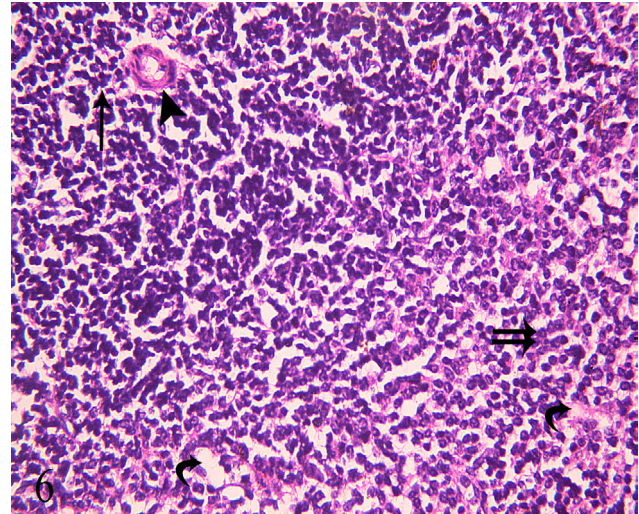


Fig. 6: A photomicrograph of a section of spleen of subgroup All showing the white pulp consists of central arteriole (▲) surrounded by many lymphocytes with darkly stained nuclei (↑). The red pulp appear consists of splenic cords (↑↑) and blood sinusoids (curved arrow). H&E. X 400.

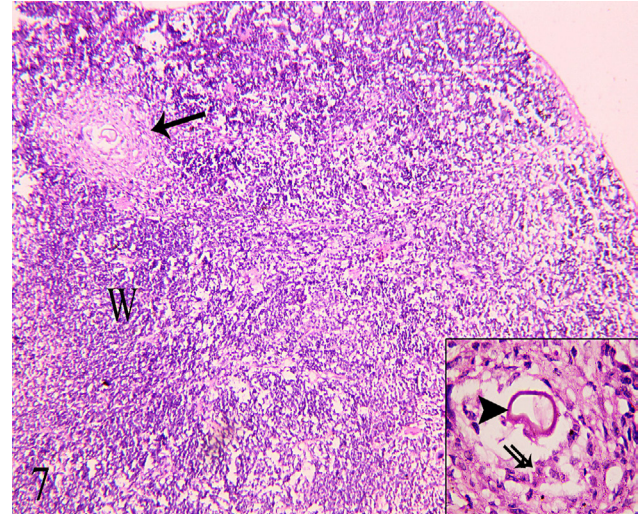


Fig. 7: A photomicrograph of a section of spleen of subgroup BI showing disrupted parenchymal architecture with loss of white pulp in some areas and other with irregular arrangement of white pulp (W). Cellular infiltration is seen surrounding Schistosoma mansoni egg (↑). Inset: Aggregation of inflammatory cells (↑↑) surrounding a degenerated egg (▲). H&E. X 100 and inset X 1000.

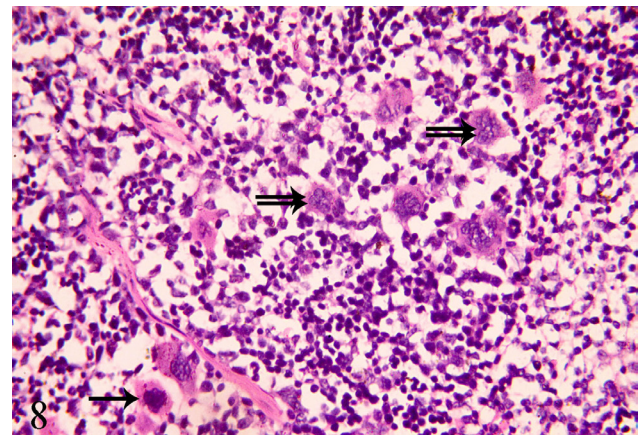


Fig. 8: A photomicrograph of a section of spleen of subgroup BI showing red pulp of spleen with megakaryocytes (↑) and giant cells (↑↑). H&E. X 400.

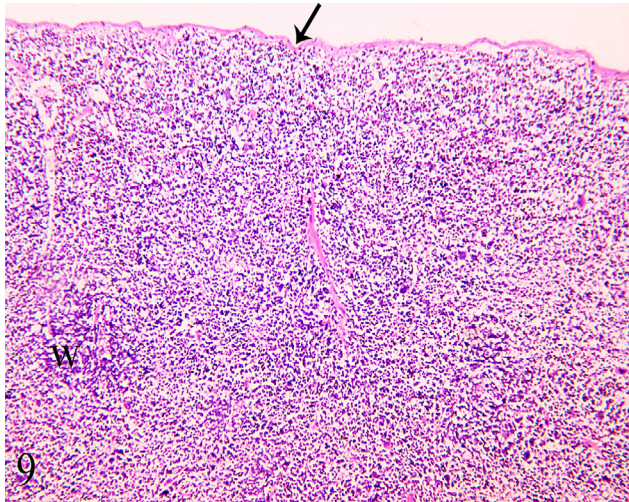


Fig. 9: A photomicrograph of a section of spleen of subgroup BII showing irregular capsule (↑) and the parenchyma is formed mainly of red pulp with reappearance of white pulp (W). H&E. X 10.

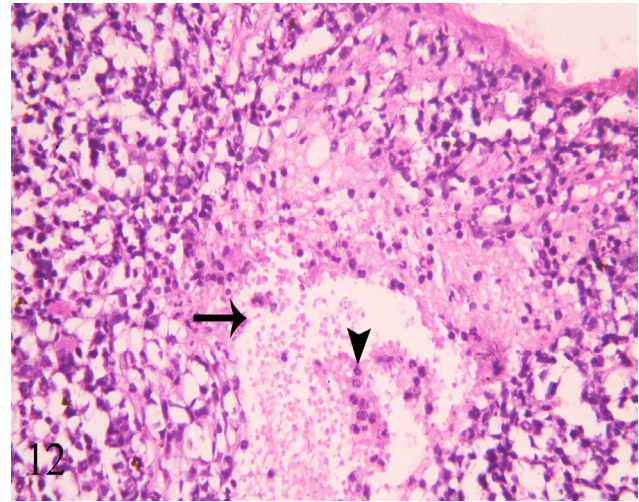


Fig. 12: A photomicrograph of a section of spleen of subgroup BIII showing disruption of the wall of the splenic vessel (↑). Notice eosinophilic material and numerous inflammatory cells (▲). H&E. X 400.

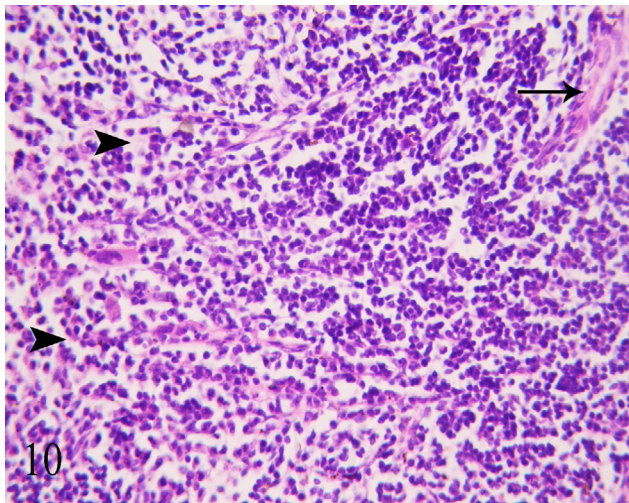


Fig. 10: A photomicrograph of a section of spleen of subgroup BII showing part of white pulp containing central arteriole (↑) and red pulp with splenic sinusoids (▲). H&E. X 400.

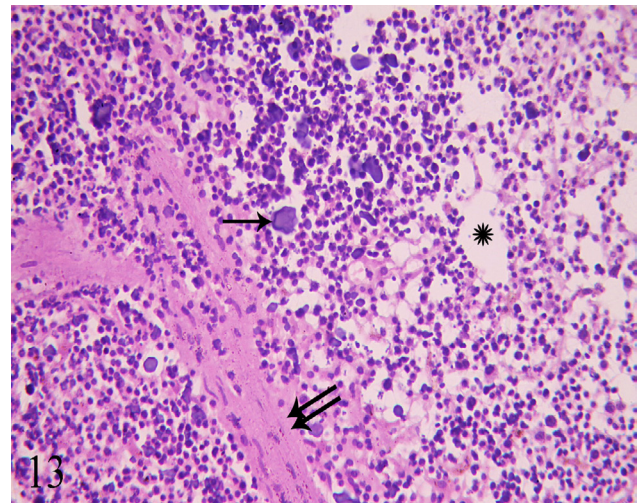


Fig. 13: A photomicrograph of a section of spleen of subgroup BIII showing many deeply basophilic calcified Schistosoma mansoni eggs with noticeable egg shell (↑) present in splenic parenchyma. Thick connective tissue septa (↑↑) and dilated splenic sinusoids (*) are detected. H&E. X 400.

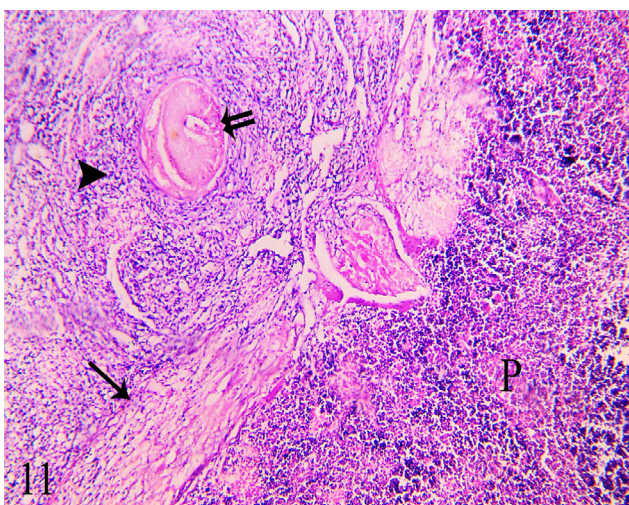


Fig. 11: A photomicrograph of a section of spleen of subgroup BIII showing Schistosoma mansoni worm (↑↑) in a blood vessel in the splenic stroma. The worm is surrounded by numerous inflammatory cells (▲). Notice thick connective tissue septum (↑) and part of the splenic stroma (P). H&E. X 100.

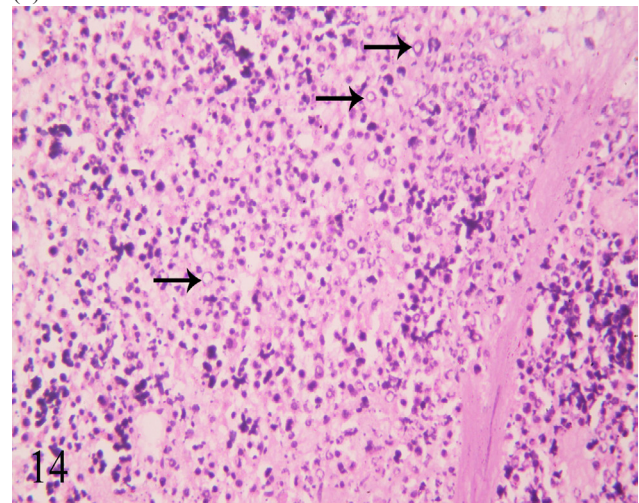


Fig. 14: A photomicrograph of a section of spleen of subgroup BIII showing the splenic parenchyma infiltrated with numerous cells with faintly stained nuclei (↑). H&E. X 400.

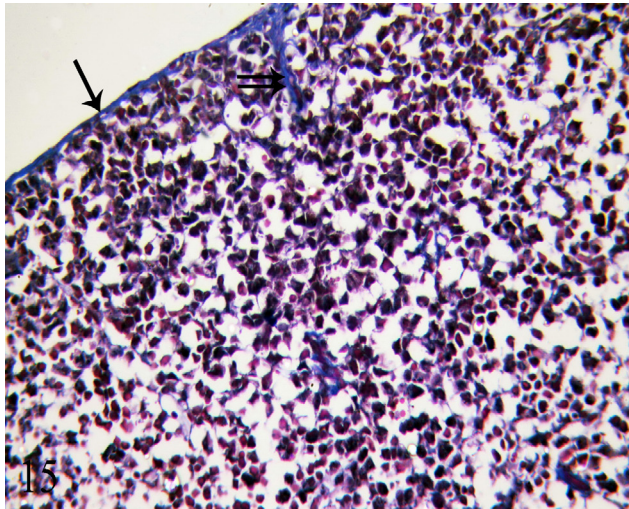


Fig. 15: A photomicrograph of a section of spleen of subgroup AII showing collagen fibers of capsule (↑) and septa (↑↑). Mallory trichrome X 400.

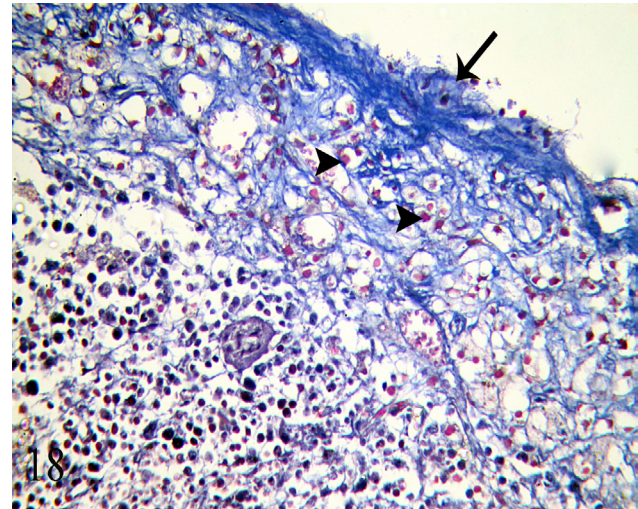


Fig. 18: A photomicrograph of a section of spleen of subgroup BIII showing apparent increase in the collagen fibers in the capsular (↑) and the subcapsular area around blood sinusoids (▲). Mallory trichrome X 400.

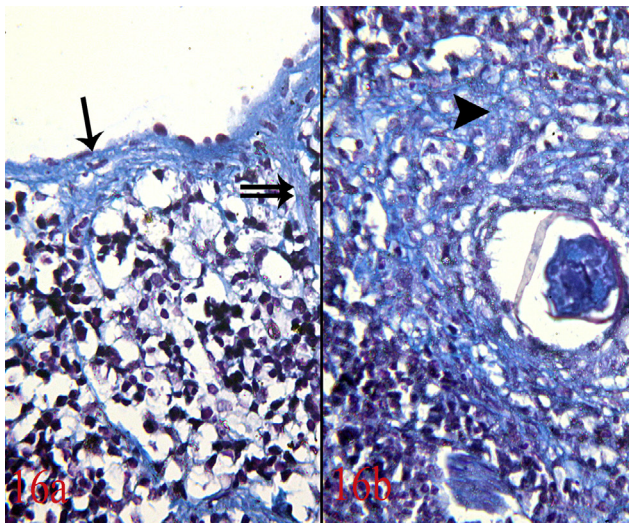


Fig. 16: A photomicrograph of a section of spleen of subgroup BI showing (a) apparent increase of collagen fibers forming the capsule (↑) and septa (↑↑). (b) collagen fibers (▲) are noticed surrounding the egg. Mallory trichrome X 400.

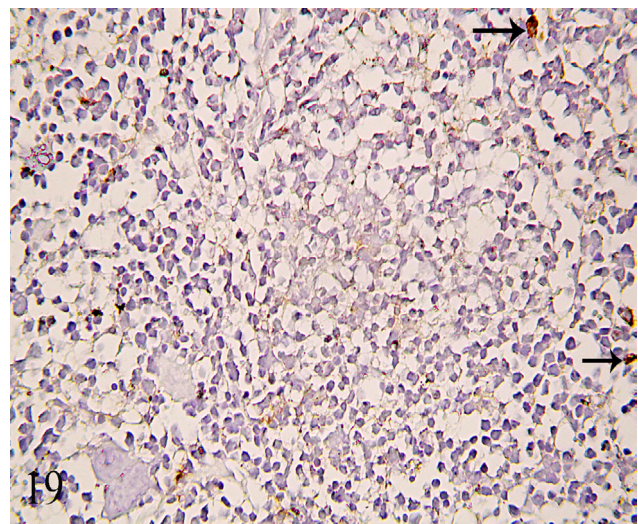


Fig. 19: A photomicrograph of a section of spleen of subgroup AII showing few scattered cells (↑) with positive immunohistochemical reaction for TNF- α . TNF- α X 400.

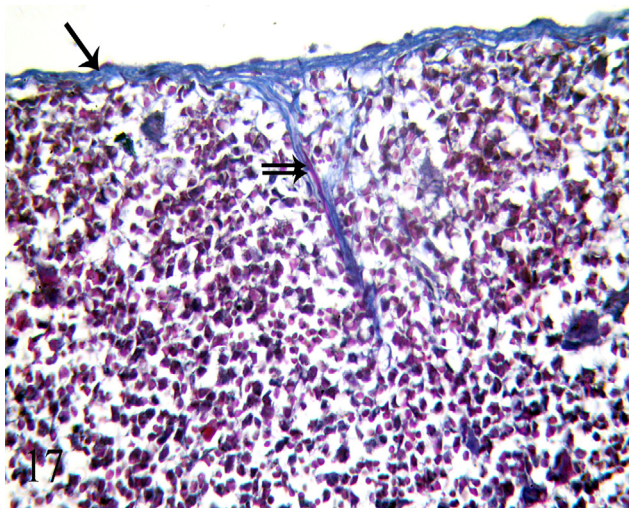


Fig. 17: A photomicrograph of a section of spleen of subgroup BII showing more or less normal collagen content of the capsule (↑) and septa (↑↑). Mallory trichrome X 400.

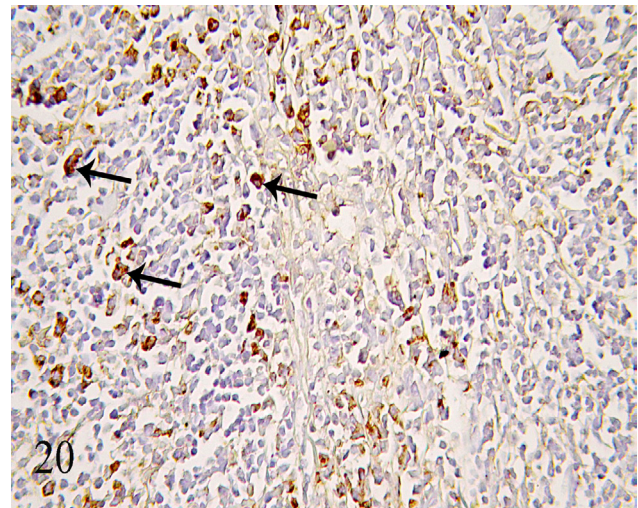


Fig. 20: A photomicrograph of a section of spleen of subgroup BI showing many cells (↑) with positive immunohistochemical reaction for TNF- α . TNF- α X 400.

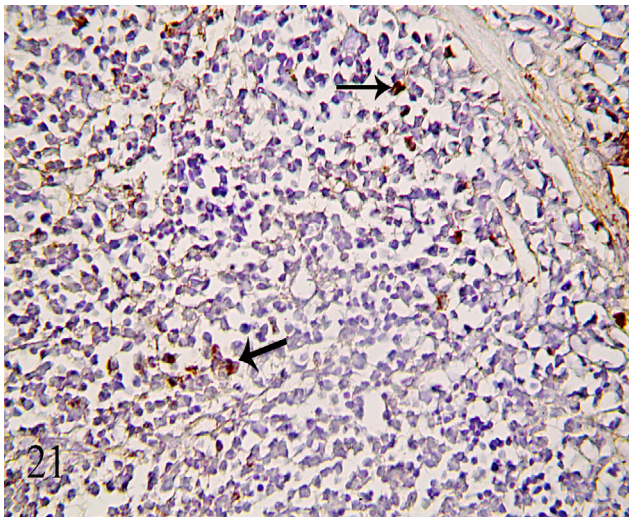


Fig. 21: A photomicrograph of a section of spleen of subgroup BII showing few cells (↑) with positive immune-histochemical reaction for TNF- α . TNF- α X 400.

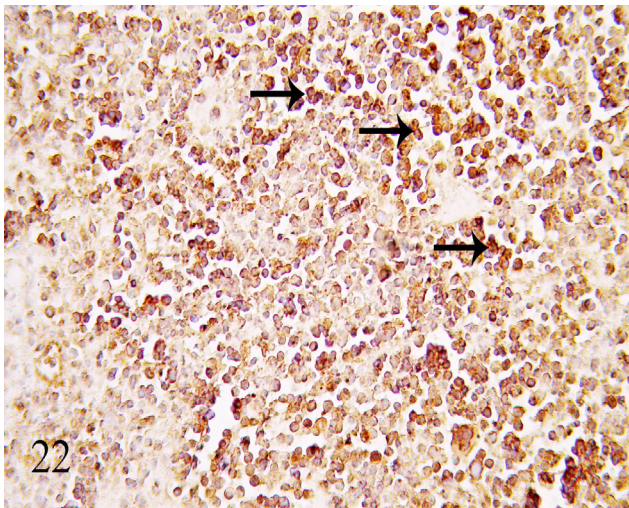


Fig. 22: A photomicrograph of a section of spleen of subgroup BIII showing numerous cells (↑) with positive immune-histochemical reaction for TNF- α . TNF- α X 400.

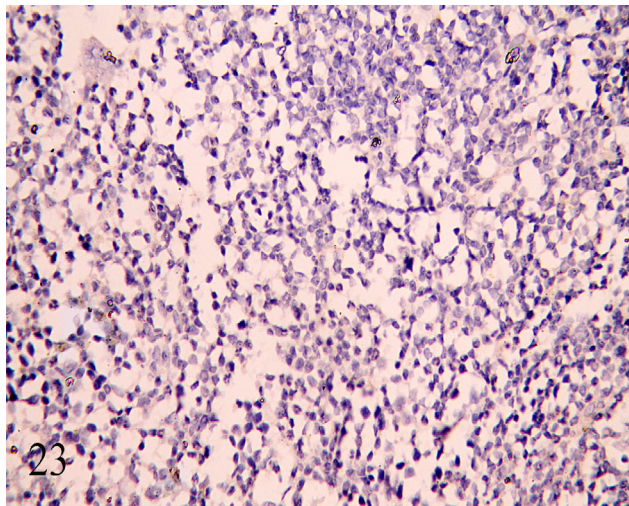


Fig. 23: A photomicrograph of a section of spleen of subgroup AII showing negative immune-histochemical reaction for CD 44. CD 44 X 400.

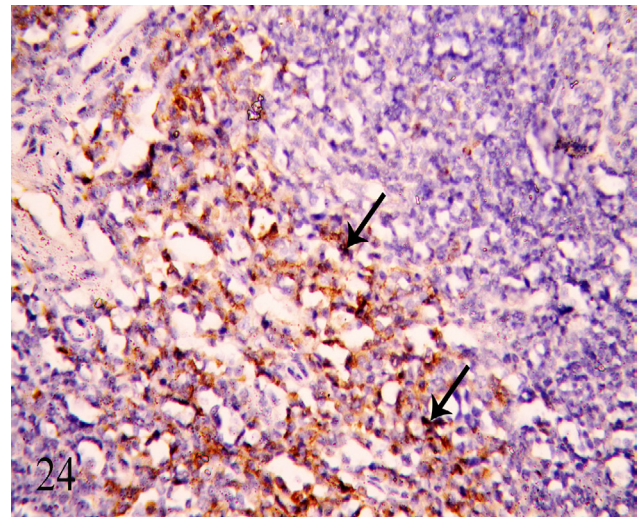


Fig. 24: A photomicrograph of a section of spleen of subgroup BII showing positive immune-histochemical reaction for CD44 (↑). CD 44 X 400.

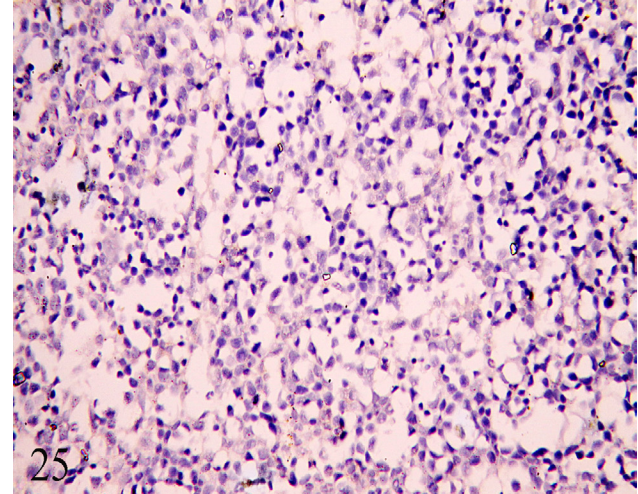


Fig. 25: A photomicrograph of a section of spleen of subgroup BIII showing negative immune-histochemical reaction for CD 44. CD 44 X 400.

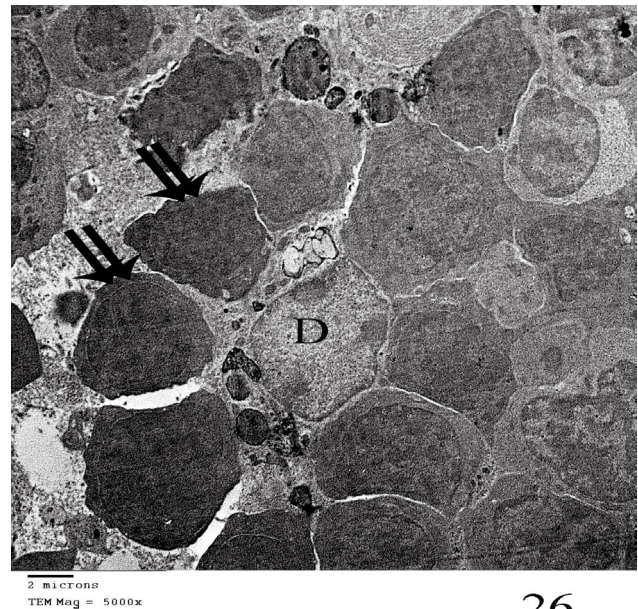


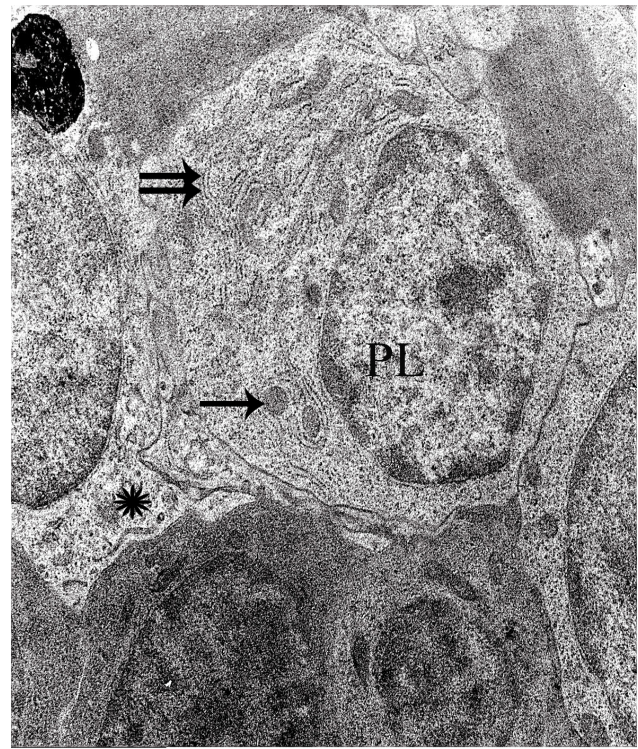
Fig. 26: An electron micrograph of a section of spleen of subgroup AII showing dendritic cell (D) and many lymphocytes (↑↑) in white pulp of the spleen. X 5000.



2 microns
TEM Mag = 12000x

27

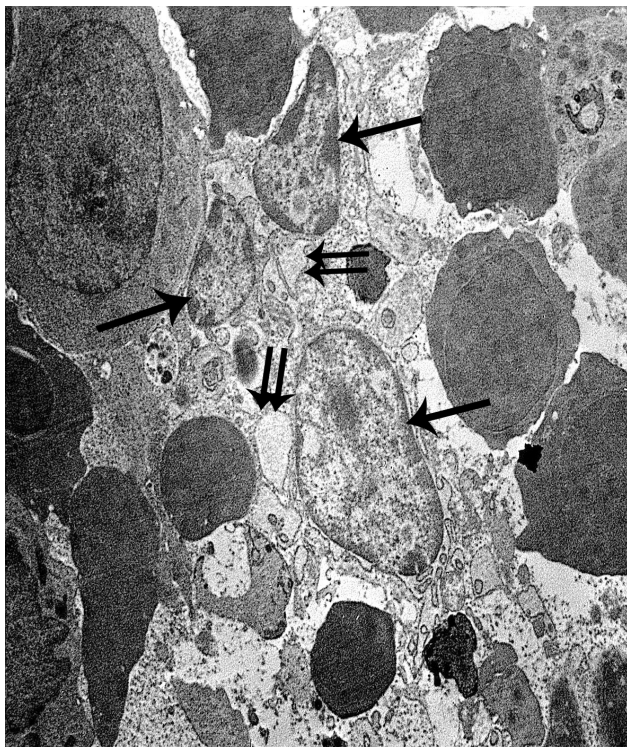
Fig. 27: A higher magnification showing a dendritic cell (D) with eccentric euchromatic nucleus and multiple cytoplasmic processes between the surrounding lymphocytes (↑). Notice the cytoplasm of the dendritic cell contains many granules with heterogenous appearances (↑↑). X 12000.



2 microns
TEM Mag = 12000x

29

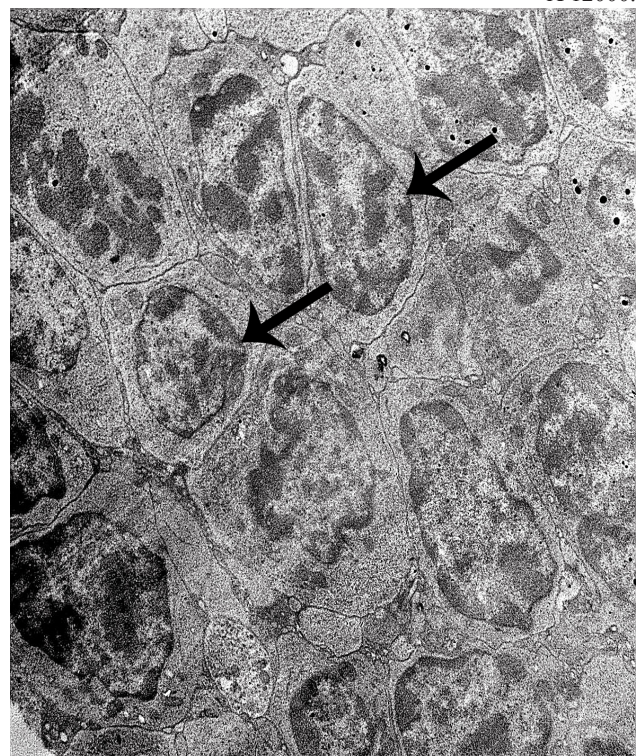
Fig. 29: An electron micrograph of subgroup AII showing plasma cell with euchromatic eccentric nuclei (PL). The cytoplasm contains well developed cisternae of rough endoplasmic reticulum (↑↑) and mitochondria (↑). Notice the cytoplasmic processes of dendritic cell (*) closely related to the plasma cell. X 12000.



2 microns
TEM Mag = 6000x

28

Fig. 28: An electron micrograph of a section of spleen of subgroup AII showing reticular cells having euchromatic nuclei (↑) with their processes surrounding electro-lucent areas (↑↑) X 6000.



2 microns
TEM Mag = 6000x

30

Fig. 30: An electron micrograph of a section of the spleen of subgroup BI showing active lymphocytes with euchromatic nuclei (↑). X 600.

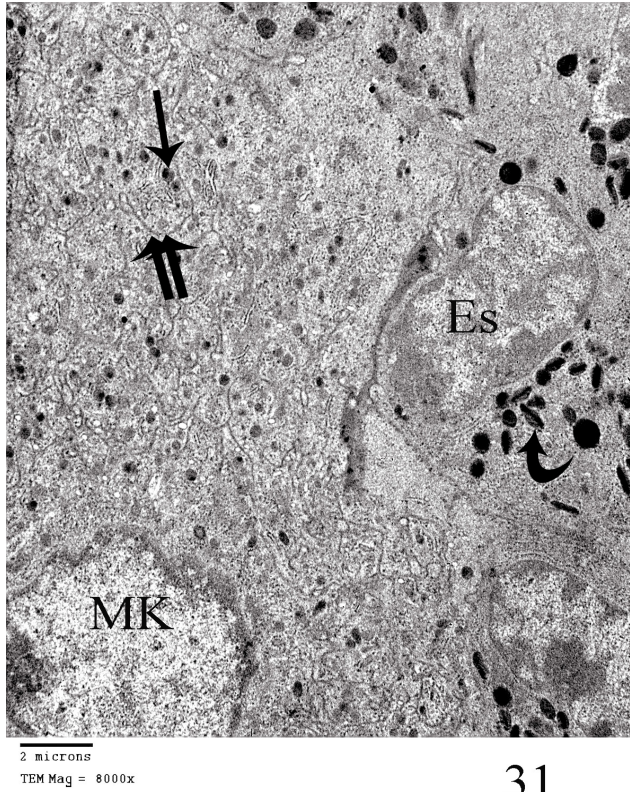


Fig. 31: An electron micrograph of a section of the spleen of subgroup BI showing part of megakaryocyte (MK) with its characteristic demarcation zones (↑↑) containing electron dense granules (↑). Notice eosinophils (Es) with their characteristic oval shaped granules (curved arrow). X8000.

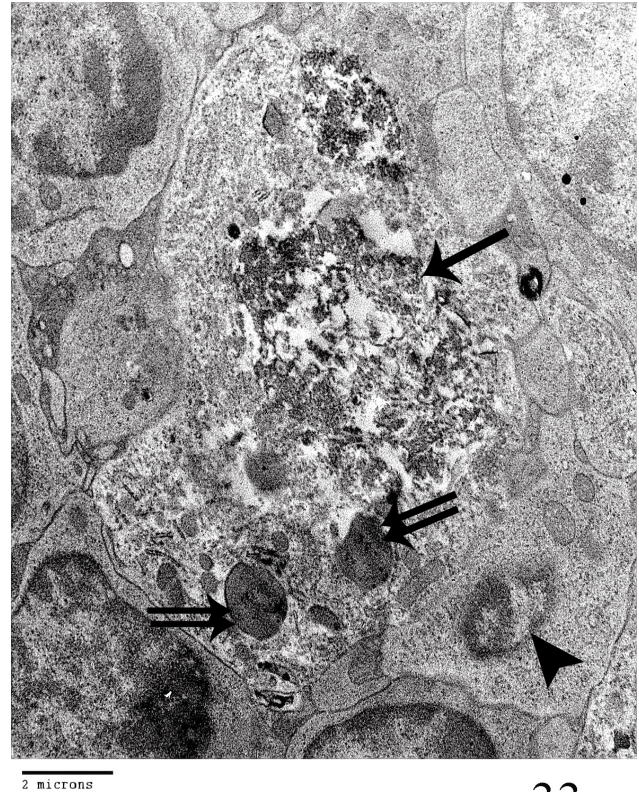


Fig. 33: An electron micrograph of a section of the spleen of subgroup BI showing a cell with fragmented nucleus with loss of the nuclear envelope (↑) and multiple electron dense granules (↑↑) in the cytoplasm. A cell with small heterochromatic nucleus is noticed (▲). X 10000.

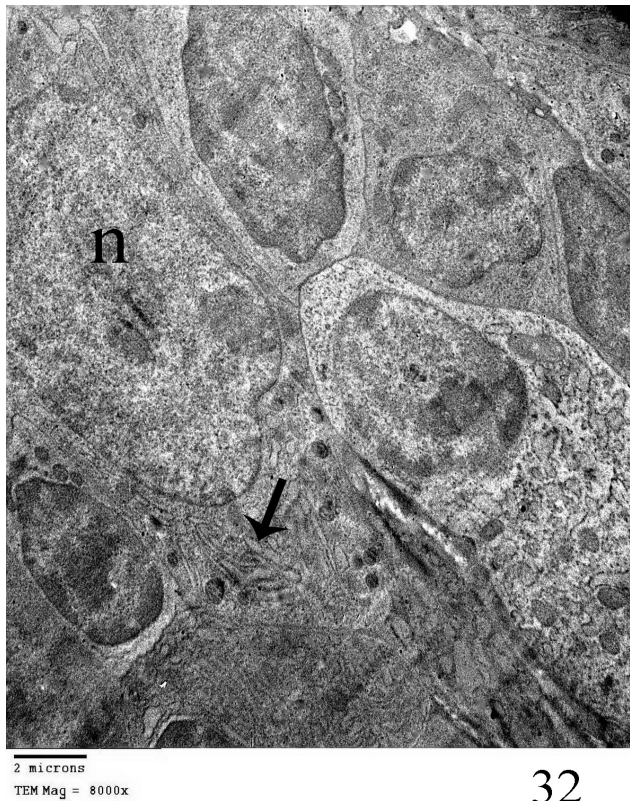


Fig. 32: An electron micrograph of a section of the spleen of subgroup BI showing a cell with euchromatic nucleus (n) and dilated cisterna of rough endoplasmic reticulum (↑) in the cytoplasm. X 8000.

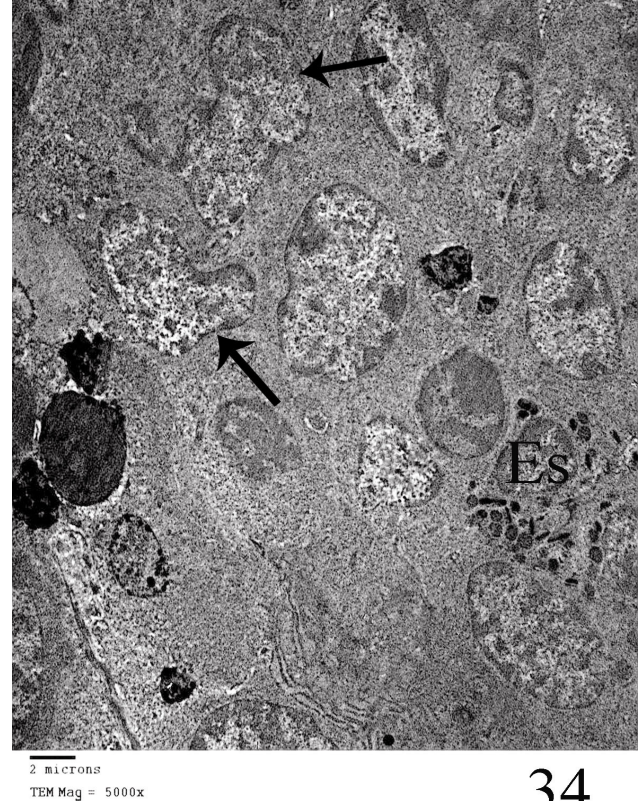
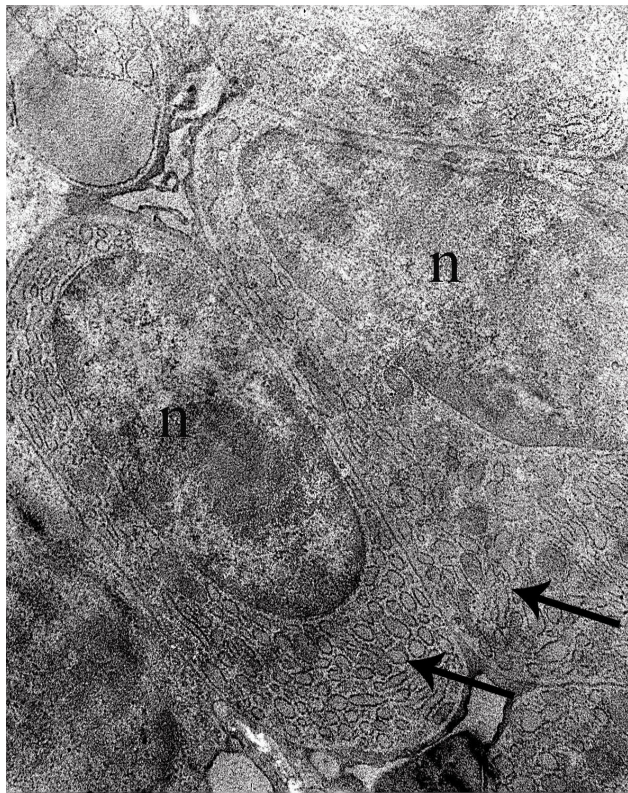


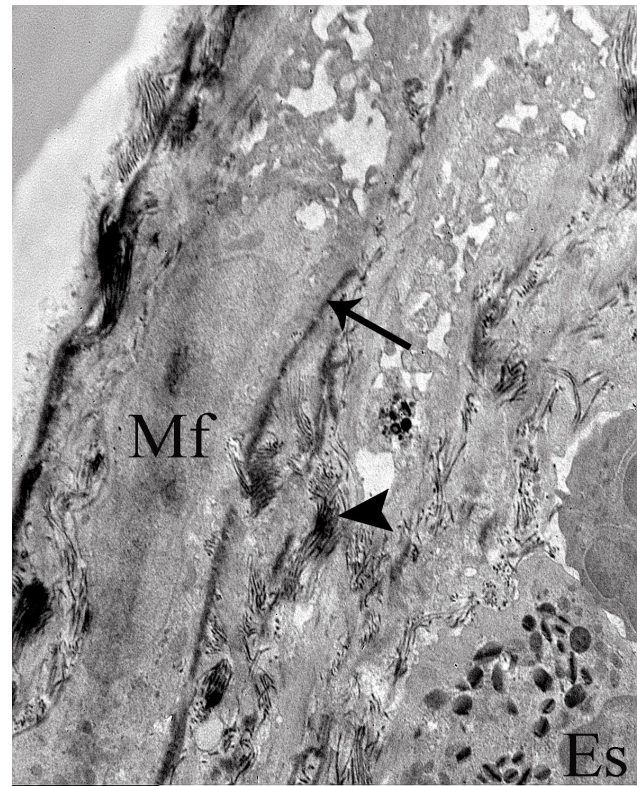
Fig. 34: An electron micrograph of a section of the spleen of subgroup BII showing cells with euchromatic nuclei and irregular nuclear membranes (↑). Notice an eosinophil (Es) with its characteristic granules. X 5000.



2 microns
TEM Mag = 12000x

35

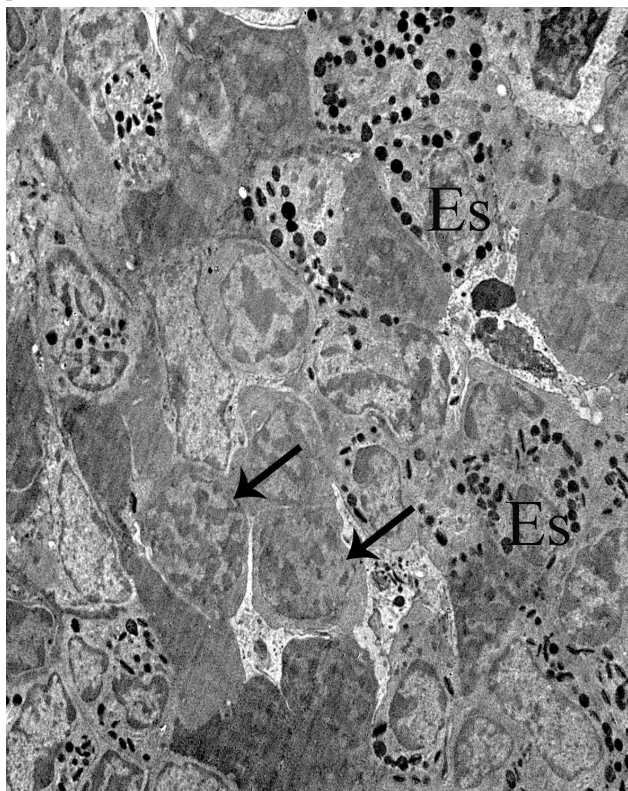
Fig. 35: An electron micrograph of a section of the spleen of subgroup BII showing cells with euchromatic nuclei (n) and prominent rER (↑) X 12000.



2 microns
TEM Mag = 8000x

37

Fig. 37: An electron micrograph of a section of the spleen of subgroup BIII showing myofibroblast (Mf) in the capsule of the spleen lying on basal lamina (↑). Notice collagen fibrils (▲) and part of eosinophil with its characteristic granules (Es). X8000.



2 microns
TEM Mag = 4000x

36

Fig. 36: An electron micrograph of a section of the spleen of subgroup BIII showing proliferating lymphocytes (↑) and numerous eosinophils (Es). X4000.

DISCUSSION

One of the most prevalent parasitic infestations is schistosomiasis. The spleen is the biggest peripheral immune organ and plays a vital role in the immune response to blood circulation. Although, it is one of the major organs affected in schistosomiasis, its structural changes have been linked to portal hypertension. In the present study, we have conducted our experiment on female mice as it has been revealed that schistosomiasis is an immune-related disease and female mice can express prominent levels of immune response due to estrogen hormone. On the contrary, androgen of male has negative effect on immune response^[19, 20]. In the present work, light microscopic examination of sections of subgroup BI displayed eggs deposition in the splenic parenchyma which was disrupted. The eggs were degenerated and surrounded by mononuclear cellular infiltration forming a granuloma. Some megakaryocytes and giant cells were also noticed as a defense mechanism. Moreover, ultrastructural examination of the same group revealed eosinophils and active lymphocytes. Some cells with many dilated cisternae of rough endoplasmic reticulum denoting activated cells secreting cytokines and cells with degenerative changes were also detected. These results were in accordance with^[21,22] who explained that eggs deposition constitutes the major

pathogenesis of schistosomiasis, with egg-laying beginning four weeks after infestation and reaching a peak at eight weeks post-infestation. Furthermore, Skelly^[23] postulated that in contrast to the adult worms, parasite eggs via soluble egg antigen (SEA) provoked a potent chemotactic activity and strong inflammatory reaction resulting in stimulation of inflammatory cells and cytokines (including interferon- γ , TNF- α and ILs). Consequently, the egg was surrounded by a variety of immune cells to form a unit called a granuloma. T helper1 (Th1), macrophages, giant cells and fibroblasts can all contribute to the granuloma formation^[22]. However, others^[24] postulated that dendritic cells were central players in the control of developing immune responses. Several main subpopulations of dendritic cells exist; immature type which is a phagocytic cell and other mature type which is not phagocytic but acts as an antigen presenting cell. At initial stages of the infestation, mature dendritic cells release IL12 which promote (Th1) differentiation and proliferation. Moreover, dendritic cells present antigen to (Th1) which consequently attract phagocytic cells by chemokines. Meanwhile, (Th1) release cytokines like γ -interferon to activate phagocytic cells. Accordingly, (Th1) mediate inflammation and macrophage activation in the initial stages of *Schistosoma* infestation. Moreover, secretory dendritic cells were also identified in our study this was in accordance with other researchers^[25] who suggested that plasmacytoid dendritic cells could arise from mature dendritic cells under the effect of inflammatory stimuli like parasitic or viral infections and this will result in the production of type I γ -interferons which enhance the function of natural killer, B and T cells. However, some researchers^[26] revealed that *Schistosoma mansoni* synthesizes glycoconjugates which interact with galectin-3; that regulates B cell differentiation into plasma cells; eliciting an intense humoral immune response. Recently, other investigators^[27] stated that megakaryocytes were present in considerable number in spleen in schistosomiasis as the platelets can play important roles in host defense against schistosome infection by directly damaging the parasites. Meanwhile, Bogers *et al.*^[28] mentioned that during hepatic and splenic schistosomiasis many eosinophils could be distinguished as their phagocytic activity which was mainly directed to the capture of antigen-antibody complexes. Moreover, Ji *et al.*^[29] stated that severe disruption of lymphoid follicles was observed at the eighth weeks post-infection as consequence of granuloma and their results were in accordance with our results. They related the loss of white pulp to the reduction of splenic lymphocytes, via apoptosis which was confirmed by the fragmentation of the nuclei in some cells in our work or the migration of the cells from the spleen to the liver. Alternatively, the increase in monocytes concurrent with splenomegaly can also destroy the splenic architecture^[30]. With time, a fibrotic reaction predominates which is formed of fibroblasts,

connective tissue fibers and dead schistosome embryo at the core of the granuloma^[31]. This was in accordance with our results as there was a significant increase in area % of collagen fibers in the granulomatous reaction surrounding a degenerated egg. According to the opinion of Hogan *et al.*^[32] TNF- α is a highly pleiotropic cytokine, with extensive biological effects. It enhances the function of antigen presenting cells, and activates monocytes. Consequently, this promotes the recruitment of macrophages, T and B cells, and eosinophils to viable ova, to form granulomas. It also upregulates extracellular matrix proteins production and collagen deposition consequently it is influential in granuloma development. This was supported by the significant increase in number of positive α -TNF cells observed in our study in the spleen of subgroup BI compared to the control.

In the current study, histological examination of sections in subgroup BIII revealed disruption of white pulp of spleen with loss of granuloma formation. Instead, the granulomas were replaced by leucocytic (eosinophils) infiltration. This was in accordance with other investigators^[21] as they explained that as the disease advances from the acute to the chronic stage, granulomas decrease in both size and cellularity because of immune regulation. Classically, the host initially responds with a (Th1) response which was directed against initial stages of the parasite. As the disease progressed, there was a switch from Th1 to Th2 response which was a hallmark of chronic schistosomiasis. Disease progression was also characterized by an increasing dominance of Th2 cytokines (IL-4, IL-5, IL-10, IL-13 and TNF- α)^[33]. Moreover, other investigators^[25,34] postulated that dendritic cells at chronic stage of the disease had a role in the shift of activation of Th1 to Th2 cell. They produced IL-10 which inhibited IL-12 production leading to inhibition of Th1. Furthermore, (SEA) might cause shift of immune response to Th2. Also, this antigen had promoted leucocyte chemotactic activity especially eosinophils^[23] and this was in accordance with our results. However, eosinophils were responsible for the cytokine profiles which had been attributed to a Th1 to Th2 shift. The numerical dominance of eosinophils could result from several factors, including enhanced proliferation of eosinophils' precursors or enhanced survival^[35].

On the other hand, the present study revealed the presence of cells with faintly stained nuclei and with margination of the chromatin at the nuclear membrane. Similar picture was detected by some investigators^[36] and they correlated this to highly proliferative tumor cells. In addition, the present work showed dilatation and disruption of the wall of the splenic vessels which contained eosinophilic material and numerous inflammatory cells. This was in accordance with^[37] as they suggested that these changes were probably due

to portal hypertension and as a response to chronic passive congestion and increased blood pressure within the splenic vessels. Moreover, some researchers^[38] hypothesized that TNF- α was expressed by both Th1 and Th2 type cells. TNF- α was a key proinflammatory molecule that increases local blood flow, up-regulates adhesion molecules on the vascular endothelium with extravasation of leukocytes. They added that TNF- α also caused activation of reticular cells. However, the egg cuticle (composed of cross-linked proteins) encloses a larva that releases enzymes and antigens through multiple pores. This would induce oxidative stress due to production of reactive oxygen species (ROS). Moreover, eosinophils generated the superoxide anion and hydroxyl radical. The ultimate result of ROS generation may be the killing of the parasite eggs and this was in accordance with our findings which revealed the presence of many deeply basophilic calcified eggs in the splenic parenchyma. However, the processes were potentially harmful for the host. The production of ROS may also initiate fibrogenesis^[39]. Meanwhile, IL-13 released from Th-2 played a significant role in the development of fibrosis as it stimulated collagen production from fibroblasts and procollagen I and II mRNA expression^[40]. These results were in accordance with our findings as there were significant increase in area % of collagen fibers in subgroup BIII compared to other subgroups. Consequently, the dilated splenic vessels and sinusoids with increase in the thickness of splenic septa and dominance of red pulp had led to splenomegaly. Other investigators^[41] explained that, pathogenesis of spleen in Schistosomiasis included two main factors: at early stage of the disease it was lymphoproliferative or cellular-proliferative which is immunologically induced and that during the late stages, a fibro-congestive appearance predominates.

In the present study, bone marrow mesenchymal stem cells (BMSCs) were injected intraperitoneally. Their existence was detected by the presence of positive CD-44 cells in the splenic sections.

In the present work, subgroup BII (BMSCs-treated group) exhibited a relative improvement in the histological picture of the spleen compared to subgroups BI and BIII. The splenic parenchyma showed few aggregations of lymphocytes forming white pulp containing central arterioles. Ultrastructural examination revealed cells with euchromatic nuclei and irregular nuclear membrane and others appeared with euchromatic nuclei and prominent rER. Some scientists^[42] reported that injured tissues can secrete chemotactic factors to recruit mesenchymal stem cells (MSCs) and the numbers of MSCs homing to the injured tissues have been shown to be independent of the route of MSCs infusion. Furthermore, some investigators^[43,44] reported that stem cell differentiation was accompanied by simultaneous changes in nuclear

mechanical properties due to the various expression of nucleo-skeleton components and the nuclei became more pliable. They explained that the chromatin in stem cells was relatively loose and showed fluid like characteristics which was attributed to low lamin A/C expression. As a result, stem cells can readily migrate through solid tissues by remodeling their cellular and nuclear morphology, while accommodating many active genes in their nuclear interior^[45]. Moreover, other researchers^[46,47] elucidated that MSCs could exert widespread immunomodulatory effects on cells of both the innate and adaptive immune system either by cell-cell contact or secretory proteins including (IL-10 and PGE-2). Mesenchymal stem cells elicit their immunomodulatory effects by inhibiting lymphocytes and dendritic cells activation and proliferation, forbidding the secretion of proinflammatory cytokines (IL12 and γ -interferon), limiting the function of antigen presenting cells, and inducing regulatory T (T-reg), B (B-reg) and dendritic (D-reg) cells which have significant roles in maintaining immune tolerance. They added that (D-reg) cells are also capable of secreting IL-10 which is a powerful anti-inflammatory cytokine and trigger the generation of (T-reg) cells. Moreover, treatment with MSCs has been shown to inhibit collagen deposition^[48] and the inhibitory effect of MSCs on the collagen deposition may be related to an enhancement of fibrotic degradation through increase the expression levels of matrix metalloproteinase (MMP) which directly degrades the extracellular matrix rather than a decrease in fibrosis synthesis^[49,50]. These findings were in accordance with our results as there was a significant decrease of number of TNF- α positive cells and area % of collagen fibers compared to subgroups BI and BIII.

CONCLUSION AND RECOMMENDATIONS

Our previous findings showed that chronic *Schistosoma mansoni* infestation has a deleterious effect on the structure of the spleen. However, BMSCs have a relevant therapeutic potential on the spleen of an animal model of *Schistosoma mansoni*. Bone marrow mesenchymal stem cells have emerged as promising candidates for cell therapy and might have a valuable role in the treatment of such endemic parasitic disease.

It is recommended to do further studies to know the exact role of MSCs and fate in treatment of splenic injuries. Timing of cell administration and the threshold number of transplanted cells should also undergo extensive investigations in long term studies before application in the clinical field.

CONFLICT OF INTEREST

There are no conflicts of interest.

REFERENCES

1. King, C.H., Dangerfield-Cha, M. The unacknowledged impact of chronic schistosomiasis. *Chronic Illn.* 2008;4, 65–79.
 2. Steinmann, P., Keiser, J., Bos, R., Tanner, M., Utzinger, J. Schistosomiasis and water resources development: systematic review, meta-analysis, and estimates of people at risk. *Lancet Infect. Dis.* 2006;6, 411–425.
 3. Quack, T., Beckmann, S. and Grevelding, C.G. Schistosomiasis and the molecular biology of the male-female interaction of *S. mansoni*. *Berl. Munch. Tierarztl. Wochenschr.*, 2006;119: 365–372.
 4. Al Sherbiny, M., Osman, A., Barakat, R., El Morshedy, H., Bergquist, R. and Olds, R. In vitro cellular and humoral responses to *Schistosoma mansoni* vaccine candidate antigens. *Acta Trop.* 2003; 88: 117–130.
 5. Xiao SH, Mei JY, Jiao PY. *Schistosoma japonicum*-infected hamsters (*Mesocricetus auratus*) used as a model in experimental chemotherapy with praziquantel, artemether, and OZ compounds. *Parasitol Res* 2011;108:431-437.
 6. Ross AG, Bartley PB, Sleight AC, Olds GR, Li Y, Williams GM, McManus DP. Schistosomiasis. *N Engl J Med* 2002;346:1212-1220.
 7. Aly HF, Mantawy MM. Efficiency of ginger (*Zingbar officinale*) against *Schistosoma mansoni* infection during host parasite association. *Parasitology International.* 2013;62: 380-389.
 8. Mostafa OM, Soliman MI. Ultrastructure alterations of adult male *Schistosoma mansoni* harbored in albino mice treated with Sidr honey and/or *Nigella sativa* oil. *Journal of King Saud University-Science* 2010;22: 111-121.
 9. Nadig RR. Stem cell therapy—hype or hope? A review. *J Conserv Dent.* 2009;12:131–138.
 10. Rountree CB, Mishra L, Willenbring H. Stem cells in liver diseases and cancer: recent advances on the path to new therapies. *Hepatology.* 2012;55:298–306.
 11. El-Badri N, Ghoneim MA. Mesenchymal stem cell therapy in diabetes mellitus: progress and challenges. *J Nucleic Acids.* 2013: 194858.
 12. Nishimura K, Takahashi J. Therapeutic application of stem cell technology toward the treatment of Parkinson's disease. *Biol Pharm Bull.* 2013;36:171–175.
 13. Trivedi P, Tray N, Nguyen T, Nigam N, Gallicano GI. Mesenchymal stem cell therapy for treatment of cardiovascular disease: helping people sooner or later. *Stem Cells Dev.* 2010;19:1109–1120.
 14. Martínez-Morales PL, Revilla A, Ocaña I, González C, Sainz P, McGuire D, Liste I. Progress in stem cell therapy for major human neurological disorders. *Stem Cell Rev.* 2013;9:685–699.
 15. Zhang Y, Mi JY, Rui YJ, Xu YL, Wang W. Stem cell therapy for the treatment of parasitic infections: is it far away? *Parasitol Res.* 2014;113(2):607-12.
 16. Abdel Aziz M, Atta H, Roshdy N, Rashed L, Sabry D, Hassouna A, Aboul Fotouh G, Hasan N, Younis R, Chowdhury J. Amelioration of Murine *Schistosoma mansoni* Induced Liver Fibrosis by Mesenchymal Stem Cells. *J Stem Cells Regen Med.* 2012 Apr 14;8(1):28-34.
 17. Alhadlaq A, Mao JJ. Mesenchymal stem cells: isolation and therapeutics. *Stem Cells Dev* 2004; 13:436–448.
 18. Bancroft JD, Layton C, Suvarna SK. *Bancroft's Theory and Practice of Histological Techniques.* 7th ed. Elsevier Churchill Livingstone: London, United Kingdom; 2013. pp. 386–535.
 19. Eloi-Santos, S., Olsen, N. J., Correa-Oliveira, R., and Colley, D. G. *Schistosoma mansoni*: Mortality, pathophysiology, and susceptibility differences in male and female mice. *Experimental Parasitology* 1992; 75, 168–175.
 20. Nakazawa M, Fantappie MR, Freeman GL Jr, Eloi-Santos S, Olsen NJ, Kovacs WJ, Secor WE, Colley DG. *Schistosoma mansoni*: susceptibility differences between male and female mice can be mediated by testosterone during early infection. *Exp Parasitol.* 1997 Mar;85(3):233-40.
 21. Wang Y, Zhang J, Yin J, Shen Y, Wang Y, Xu Y, Cao J. The formation of egg granulomas in the spleens of mice with late *Schistosoma japonicum* infection alters splenic morphology. *Parasit Vectors.* 2015 Jul 16;8:375.
 22. Pearce EJ, MacDonald AS. The immunobiology of schistosomiasis. *Nature reviews.* 2002;2:499–511.
 23. Skelly PJ. The use of imaging to detect schistosomes and diagnose schistosomiasis. *Parasite Immunol.* 2013 Sep-Oct;35(9-10):295-301.
 24. Hey YY and O'Neill HC. Murine spleen contains a diversity of myeloid and dendritic cells distinct in antigen presenting function. *J Cell Mol Med.* 2012 Nov;16(11):2611-9.
 25. Perona-Wright G, Jenkins SJ, MacDonald AS. Dendritic cell activation and function in response to *Schistosoma mansoni*. *Int J Parasitol.* 2006 May 31;36(6):711-21.
 26. Brand C, Oliveira FL, Takiya CM, Palumbo A Jr, Hsu DK, Liu FT, Borojevic R, Chammas R, El-Cheikh MC.
-

- The involvement of the spleen during chronic phase of *Schistosoma mansoni* infection in galectin-3^{-/-} mice. *Histol Histopathol.* 2012 Aug;27(8):1109-20.
27. Akram A, Da'dara, Patrick J, Skelly. Schistosomes versus platelets. *Thrombosis Research.* 2014;134(6):1176-1181.
 28. Bogers JJ, Nibbeling HA, Deelder AM, van Marck EA. Immunohistochemical and ultrastructural localization of *Schistosoma mansoni* soluble egg antigens processed by the infected host. *Parasitology.* 1996 Jun;112 (Pt 6):537-43.
 29. Ji F, Liu Z, Cao J, Li N, Liu Z, Zuo J, Chen Y, Wang X, Sun J. B. Cell response is required for granuloma formation in the early infection of *Schistosoma japonicum*. *PLoS One.* 2008 Mar 5;3(3):e1724.
 30. Kurt RA, Brault MS, Fried B. Evidence of altered secondary lymphoid-tissue chemokine responsiveness in Balb/c mice infected with *Schistosoma mansoni*. *J Parasitol.* 2003;89(4):721–5.
 31. Grimaud JA, Borojevic R. Portal fibrosis: intrahepatic portal vein pathology in chronic human schistosomiasis *mansoni*. *Journal of submicroscopic cytology.* 1986; 18:783–793.
 32. Hogan LH, Wang M, Suresh M, Co DO, Weinstock JV, Sandor M. CD4⁺ TCR repertoire heterogeneity in *Schistosoma mansoni*-induced granulomas. *J Immunol* 2002; 169:6386–93.
 33. Fairfax K, Nascimento M, Huang SC, Everts B, Pearce EJ. Th2 responses in schistosomiasis. *Semin Immunopathol.* 2012;34(6):863–71.
 34. Shaler CR, Kugathasan K, McCormick S, Damjanovic D, Horvath C, Small CL, et al. Pulmonary mycobacterial granuloma increased IL-10 production contributes to establishing a symbiotic host-microbe microenvironment. *Am J Pathol.* 2011;178(4):1622–34.
 35. Rumbley CA and Phillips SM. The schistosome granuloma: an immunoregulatory organelle. *Microbes Infect.* 1999 Jun;1(7):499-504.
 36. Ip YT, Dias Filho MA, Chan JK. Nuclear inclusions and pseudoinclusions: friends or foes of the surgical pathologist? *Int J Surg Pathol.* 2010 Dec;18(6):465-81.
 37. Freitas CR, Barbosa AA Jr, Fernandes AL, Andrade ZA. Pathology of the spleen in hepatosplenic schistosomiasis. Morphometric evaluation and extracellular matrix changes. *Mem Inst Oswaldo Cruz.* 1999 Nov-Dec;94(6):815-22.
 38. Booth M, Mwatha JK, Joseph S, Jones FM, Kadzo H, Ileri E, Kazibwe F, Kemijumbi J, Kariuki C, Kimani G, Ouma JH, Kabatereine NB, Vennervald BJ, Dunne DW. Periportal fibrosis in human *Schistosoma mansoni* infection is associated with low IL-10, low IFN-gamma, high TNF-alpha, or low RANTES, depending on age and gender. *J Immunol.* 2004 Jan 15;172(2):1295-303.
 39. El-Sokkary GH, Omar HM, Hassanein AF, Cuzzocrea S, Reiter RJ. Melatonin reduces oxidative damage and increases survival of mice infected with *Schistosoma mansoni*. *Free Radic Biol Med.* 2002 Feb 15;32(4):319-32.
 40. Chiamonte, M. G., M. Mentink-Kane, B. A. Jacobson, A. W. Cheever, M. J. Whitters, M. E. P. Goad, A. Wong, M. Collins, D. D. Donaldson, M. J. Grusby, and T. A. Wynn. Regulation and function of the interleukin 13 receptor alpha 2 during a T helper cell type 2-dominant immune response. *J. Exp. Med.* 2003;197:687–701.
 41. Teixeira-Carvalho A, Martins-Filho OA, Andrade ZA, Cunha-Mello JR, Wilson RA, Correa-Oliveira R. The study of T-cell activation in peripheral blood and spleen of hepatosplenic patients suggests an exchange of cells between these two compartments in advanced human *Schistosomiasis mansoni* infection. *Scand J Immunol.* 2002 Sep;56(3):315-22.
 42. Herrera MB, Bussolati B, Bruno S, Morando L, Mauriello-Romanazzi G, Sanavio F, Stamenkovic I, Biancone L, Camussi G. Exogenous mesenchymal stem cells localize to the kidney by means of CD44 following acute tubular injury. *Kidney Int* 2007;72:430–41.
 43. Pekovic, V., & Hutchison, C J. Adult stem cell maintenance and tissue regeneration in the ageing context: the role for A-type lamins as intrinsic modulators of ageing in adult stem cells and their niches. *Journal of Anatomy,* 2008: 213(1), 5–25.
 44. Righolt CH, van 't Hoff ML, Vermolen BJ, Young IT, Raz V. (2011). Robust nuclear lamina- based cell classification of aging and senescent cells. *Aging,* 2011:3(12),1192–1201.
 45. Hampoelz, B., & Lécuit, T. Nuclear mechanics in differentiation and development. *Current Opinion in Cell Biology,* 2011:23(6), 668–675.
 46. Ma OK, Chan KH. Immunomodulation by mesenchymal stem cells: Interplay between mesenchymal stem cells and regulatory lymphocytes. *World J Stem Cells.* 2016 Sep 26;8(9):268-78.
 47. Liu WH, Liu JJ, Wu J, et al. Novel mechanism of inhibition of dendritic cells maturation by mesenchymal stem cells via interleukin-10 and the JAK1/ STAT3 signaling pathway. *PLoS One* 2013;8:e55487.

48. Pan, RL, Wang, P, Xiang, LX and Shao, JZ. Delta-like 1 serves as a new target and contributor to liver fibrosis down-regulated by mesenchymal stem cell transplantation. *J Biol Chem.* 2011 Apr 8; 286 (14): 12340–12348.
49. Xu H, Qian H, Zhu W, Zhang X, Yan Y, Mao F, Wang M, Xu H, Xu W. Mesenchymal stem cells relieve fibrosis of *Schistosoma japonicum*-induced mouse liver injury. *Exp Biol Med (Maywood).* 2012 May;237(5):585-92.
50. Lozito, TP., Jackson, WM., Nesti, LJ. & Tuan, RS. Human mesenchymal stem cells generate a distinct pericellular zone of MMP activities via binding of MMPs and secretion of high levels of TIMPs. *Matrix Biol.* 2014;34, 132–143.

المخلص العربي

دراسة هيستولوجية على الدور العلاجي المحتمل للخلايا الجذعية الوسيطة المشتقة من نخاع العظام في نموذج للإصابة بالشيستوزوما المنسونية في طحال الفئران

منى حسين رأفت، سارة عبد الجواد، هبة فكرى

قسم الهستولوجيا وبيولوجيا الخلية - كلية الطب - جامعة عين شمس- القاهرة- مصر

المقدمة: إن تضخم الكبد والطحال هو خاصية مميزة في عدوى البلهارسيا. ومع ذلك لقد تداولت القليل من البحوث العلمية إصابة الطحال نتيجة مرض البلهارسيا على عكس إصابة الكبد المعروفة. بالإضافة الى أن دور الخلايا الجذعية الوسيطة المشتقة من نخاع العظام في علاج الطحال المصاب بالبلهارسيا لم يتم بعد التحقق منه. الهدف من البحث: استكشاف التغيرات النسيجية التي قد تحدث للطحال خلال العدوى المزمنة بالبلهارسيا والدور العلاجي المحتمل للخلايا الجذعية الوسيطة المشتقة من نخاع العظام في تحسين هذه التغييرات.

المواد وطرق البحث: تم تصنيف خمسين من أنثى فئران ألبينو السويسرية التي تزن حوالي ٢٥ جم الى المجموعة أ (المجموعة الضابطة) والمجموعة ب (المجموعة التجريبية). تم تقسيم الحيوانات في المجموعة أ بالتساوي إلى المجموعة الفرعية أ١ التي استخدمت كمصدر للخلايا الجذعية والتي تم الحصول عليها من نخاع العظام، والمجموعة الفرعية أ٢ التي تم حقنها بمحلول ملحي وتستخدم لجمع عينات الطحال الضابطة. في حين أن كل فئران المجموعة ب تم اصابتها بسيركاريا الشيستوزوما المنسونية (٦٠ / فأر) حيث حقنت تحت الجلد، ثم تم تقسيمها إلى ثلاث مجموعات فرعية؛ المجموعة الفرعية ب١ والتي تم بها التضحية بعد ثمانية أسابيع، المجموعة الفرعية ب٢ وفيها تم حقن كل فأر داخل الصفاق ٢ x ٦١٠ من الخلايا الجذعية الوسيطة المشتقة من نخاع العظام المعلقة في محلول ملحي وذلك في الأسبوع الثامن بعد العدوى ثم تم التضحية بها بعد أربعة أسابيع لاحقا، والمجموعة الفرعية ب٣ التي تركت لمدة اثني عشر أسبوعا دون علاج ثم تم التضحية بها.

النتائج: كشف الفحص الهستولوجي للطحال للمجموعة الفرعية ب١ عن تغيرات هيكلية من حيث ترسب البيض الذي كان محاط بالخلايا الالتهابية وألياف الكولاجين. اما المجموعة الفرعية ب٣ فقد أظهرت تغييرات هيكلية أكثر شدة. وقد ارتبط هذا مع زيادة نو دلالة إحصائية في ألياف الكولاجين والتفاعل المناعي لعامل نخر الورم ألفا مقارنة بالمجموعة الضابطة. اما بالنسبة للمجموعة الفرعية ب٢ (مجموعة الخلايا الجذعية الوسيطة المشتقة من نخاع العظام) فقد أظهرت تحسن في تركيب الطحال.

الاستنتاج: ان العدوى المزمنة بالبلهارسيا المنسونية لها تأثير ضار على تركيب الطحال. اما الخلايا الجذعية الوسيطة المشتقة من نخاع العظام فلديها دور علاجي وثيق الصلة على الطحال في نموذج مرض البلهارسيا المنسونية.